Commun Nonlinear Sci Numer Simulat 16 (2011) 1541–1554

Contents lists available at ScienceDirect

Commun Nonlinear Sci Numer Simulat

journal homepage: www.elsevier.com/locate/cnsns

On the Chebyshev spectral continuous time approximation for constant and periodic delay differential equations

Eric A. Butcher, Oleg A. Bobrenkov *

Department of Mechanical and Aerospace Engineering, New Mexico State University, Las Cruces, New Mexico 88003, USA

ARTICLE INFO

Article history:
Received 14 January 2010
Accepted 23 May 2010
Available online 25 June 2010

Keywords:
Chebyshev collocation
Continuous time approximation
Periodic delay differential equations

ABSTRACT

In this paper, the approximation technique proposed in Breda et al. (2005) [1] for converting a linear system of constant-coefficient delay differential equations (DDEs) into a system of ordinary differential equations (ODEs) using pseudospectral differencing is extended to linear and nonlinear systems of DDEs with time-periodic coefficients. The Chebyshev spectral continuous time approximation (ChSCTA) technique is used to study the stability of first and second-order constant coefficient DDEs, a delayed system with a cubic nonlinearity and parametric sinusoidal excitation, the delayed Mathieu's equation, and delayed systems with two fixed delays. In all the examples, the stability and time response obtained from ChSCTA show good agreement with either analytical results, or the results obtained before by other reliable approximation methods. The "spectral accuracy" convergence behavior of Chebyshev spectral collocation shown in Trefethen (2000) [2] which the proposed technique possesses is compared to the convergence properties of finite difference-based continuous time approximation for constant-coefficient DDEs proposed recently in Sun (2009) [3] and Sun and Song (2009) [4].

1. Introduction

Delay differential equations (DDEs) describe various processes in engineering, as well as in the physical and biological sciences. For many years, the behavior of delayed systems has been the subject of research. The time response and stability analysis of constant and periodic DDEs, in particular, has received much attention in the literature. References [1,3,5], for instance, present three different numerical techniques that can be used to obtain the time response or stability characteristics of constant-coefficient DDEs. One group of methods to study the stability of periodic DDEs allows converting them into maps. A Chebyshev collocation method based on the properties of Chebyshev polynomials [6] is used to discretize the monodromy operator in [7,8], while a similar technique based on pseudospectral differencing is shown in [9]. Two other methods which discretize periodic DDEs by maps are semi-discretization [10] and temporal finite element analysis [11].

Introducing the solution operator and its infinitesimal generator allows one to represent a constant DDE as an abstract ODE as in [12–14]. This representation is used in [5,1,15] in order to compute the characteristic roots. The abstract ODE obtained is first approximated using the uniform mesh of the delay period in [5] and pseudospectral differencing in [1]. In two recent papers, constant-coefficient systems of DDEs with single and multiple delays as well as nonlinear and sinusoidal forcing terms are approximated by using finite difference differentiation [3,4]. As was shown in [2], however, spectral differentiation has a higher rate of convergence than finite difference differentiation.

* Corresponding author. Tel.: +1 575 646 3501; fax: +1 575 646 6111.
E-mail addresses: eab@nmsu.edu (E.A. Butcher), chaalis@nmsu.edu (O.A. Bobrenkov).

1007-5704/$ - see front matter © 2010 Elsevier B.V. All rights reserved.
doi:10.1016/j.cnsns.2010.05.037

This paper illustrates the Chebyshev spectral continuous time approximation (ChSCTA) [16]. Its purposes are (1) to show numerically that the continuous time approximation of constant-coefficient delay DDEs based on finite differences considered in [3,4] is less accurate than ChSCTA based on spectral differentiation, (2) to extend ChSCTA to the case of time-periodic linear DDEs via the illustrative example of a delayed Mathieu equation, and (3) to extend the approach to nonlinear time-periodic DDEs. Consequently, all the techniques of stability and bifurcation analysis for continuous time systems are applicable to the equation obtained. While several collocation methods which appear in the literature are used for solving DDE initial value problems [17,18] and for finding periodic solutions of nonlinear DDEs [19], the authors believe that the use of such methods for both response and stability problems of periodic DDEs while utilizing the continuous time approximation approach (as opposed to direct discretization of the monodromy operator) is explored numerically for the first time.

For illustrative examples, we consider first and second-order constant coefficient DDEs, a delayed system with a cubic nonlinearity and parametric sinusoidal excitation, the delayed Mathieu's equation, and delayed systems with two fixed delays. It should be noted that for the case of periodic DDEs, a periodic analogue of the infinitesimal generator for constant DDEs is discretized yielding accurate stability and time response results. While the authors are aware that a complete theory for the periodic case is lacking, the main objective here is to explore this idea through numerical examples, while a possible theoretical justification for the numerical technique employed is offered in the Appendix.

2. Continuous time approximation for linear constant DDEs

2.1. Representation as abstract ODEs

Consider a system of linear constant-coefficient DDEs with a single discrete time delay described by

$$\begin{aligned}\dot{\mathbf{x}}(t) &= \mathbf{A}\mathbf{x}(t) + \mathbf{B}\mathbf{x}(t-\tau)\\ \mathbf{x}(t) &= \phi(t), \quad -\tau \leqslant t \leqslant 0\end{aligned} \tag{1}$$

where $\mathbf{x} \in \mathbb{R}^q$ is a q-dimensional state vector, $\mathbf{A}$ and $\mathbf{B}$ are constant matrices, and $\phi(t)$ is the initial vector function. As explained in [12–14], Eq. (1) can be treated as an abstract ODE

$$\dot{\mathscr{y}}(t) = \mathscr{A}\mathscr{y}(t) \tag{2}$$

where $\mathscr{y}(t)$ is an infinite-dimensional vector and $\mathscr{A}$ is the infinitesimal generator of the solution operator

$$(\mathscr{T}\phi)(\theta) = \mathscr{y}(\phi)(\theta) = \mathbf{x}(\phi)(t+\theta), \qquad \theta \in [-\tau, 0], \quad t \geqslant 0 \tag{3}$$

which maps the initial function onto the state at time t. This operator is a strongly continuous semigroup, and it satisfies all the semigroup properties. The operator $\mathscr{A}$, which satisfies

$$\mathscr{D}(\mathscr{A}) = \left\{\phi \in \mathscr{C}([-\tau,0],\mathbb{R}^n) : \frac{d\phi}{d\theta} \in \mathscr{C}([-\tau,0],\mathbb{R}^n), \dot{\phi}(0) = \mathbf{A}\phi(0) + \mathbf{B}\phi(-\tau)\right\}, \tag{4}$$

$$\mathscr{A}\phi = \frac{d\phi}{d\theta}$$

where $\mathscr{D}(\mathscr{A})$ denotes the domain of $\mathscr{A}$ and $\mathscr{C}$ is a Banach space, can be thought of as an infinite-dimensional square matrix. Approximation of the infinite dimensional vector $\mathscr{y}(t)$ and operator $\mathscr{A}$ with finite dimensional ones is the main idea of CTA.

In the next two subsections, we will review the CTA of Eq. (2) with the aid of finite difference differentiation as it was done in [3], show how this can also be done by ChSCTA, and demonstrate the advantages of the latter approach over the former. In addition, we will compare the usage of different order finite differences for the first approach.

2.2. Finite difference formulation

Consider the continuous time approximation for the constant-coefficient DDE (2) described in [3]. In this case, $\mathscr{y}(t)$ is discretized by a uniform grid on the τ-periodic interval $[t-\tau, t]$. Let N be an integer such that $\Delta\tau = \tau/N$ and $\tau_i = i\Delta\tau$ ($i = 1,2,\ldots,N$). Then, the second-order centered finite difference differentiation is used to approximate the derivatives of $\mathbf{x}(t-\tau_i)$, $1 \leqslant i \leqslant N-1$, as

$$\dot{\mathbf{x}}(t - i\Delta\tau) = \frac{1}{2\Delta\tau}[\mathbf{x}(t-(i-1)\Delta\tau) - \mathbf{x}(t-(i+1)\Delta\tau)] \tag{5}$$

while Eq. (1) is used at the boundary point $i = 0$, and a forward difference is used at $i = N$. Alternatively, by using the first-order forward finite differences, the derivatives are approximated as [3]

$$\dot{\mathbf{x}}(t - i\Delta\tau) = \frac{1}{\Delta\tau}[\mathbf{x}(t-(i-1)\Delta\tau) - \mathbf{x}(t-i\Delta\tau)] \tag{6}$$

The finite-dimensional approximation to $\mathscr{Y}(t)$ is written as

$$\mathbf{y}(t) = \begin{bmatrix}\mathbf{x}^{\mathrm{T}}(t) & \mathbf{x}^{\mathrm{T}}(t-\Delta\tau) & \mathbf{x}^{\mathrm{T}}(t-2\Delta\tau) & \cdots & \mathbf{x}^{\mathrm{T}}(t-N\Delta\tau)\end{bmatrix}^{\mathrm{T}} \equiv \begin{bmatrix}\mathbf{y}_1^{\mathrm{T}}(t) & \mathbf{y}_2^{\mathrm{T}}(t) & \mathbf{y}_3^{\mathrm{T}}(t) & \cdots & \mathbf{y}_{N+1}^{\mathrm{T}}(t)\end{bmatrix}^{\mathrm{T}} \tag{7}$$

The approximation to Eq. (2) is therefore obtained as

$$\dot{\mathbf{y}}(t) = \widehat{\mathbf{A}}_{\mathrm{fd}}\mathbf{y}(t) \tag{8}$$

where $\widehat{\mathbf{A}}_{\mathrm{fd}}$ is the finite difference-based approximation to the infinitesimal generator $\mathscr{A}$ defined by

$$\widehat{\mathbf{A}}_{\mathrm{fd}}^{c} = \begin{bmatrix} \mathbf{A} & \mathbf{0}_q & \mathbf{0}_q & \cdots & \mathbf{0}_q & \mathbf{B} \\ \frac{1}{2\Delta\tau}\mathbf{I}_q & \mathbf{0}_q & -\frac{1}{2\Delta\tau}\mathbf{I}_q & \mathbf{0}_q & \cdots & \mathbf{0}_q \\ & \ddots & & \ddots & & \\ & & \ddots & & \ddots & \\ \mathbf{0}_q & \cdots & \mathbf{0}_q & \frac{1}{2\Delta\tau}\mathbf{I}_q & \mathbf{0}_q & -\frac{1}{2\Delta\tau}\mathbf{I}_q \\ \mathbf{0}_q & \mathbf{0}_q & \cdots & \mathbf{0}_q & \frac{1}{\Delta\tau}\mathbf{I}_q & -\frac{1}{\Delta\tau}\mathbf{I}_q \end{bmatrix} \tag{9}$$

for the case of central finite difference derivative approximation. For the case of forward finite differences, the same approximation is defined by

$$\widehat{\mathbf{A}}_{\mathrm{fd}}^{f} = \begin{bmatrix} \mathbf{A} & \mathbf{0}_q & \mathbf{0}_q & \cdots & \mathbf{0}_q & \mathbf{B} \\ \frac{1}{\Delta\tau}\mathbf{I}_q & -\frac{1}{\Delta\tau}\mathbf{I}_q & \mathbf{0}_q & \cdots & \mathbf{0}_q & \mathbf{0}_q \\ & \ddots & \ddots & & & \\ & & & \ddots & \ddots & \\ \mathbf{0}_q & \mathbf{0}_q & \cdots & \mathbf{0}_q & \frac{1}{\Delta\tau}\mathbf{I}_q & -\frac{1}{\Delta\tau}\mathbf{I}_q \end{bmatrix} \tag{10}$$

It should be observed that the first q equations in (8) are identical to Eq. (1). The forward finite difference is used in the last row of $\widehat{\mathbf{A}}_{\mathrm{fd}}^{c}$ because otherwise this matrix has eigenvalues with positive real part. (Note that while the version of matrix above shown in [3] uses only forward differences, it was stated that centered differences were used in the computations). Higher-order finite differences may also be employed for increased accuracy, although this was not done in [3]. In Fig. 1 the convergence characteristics of second- and fourth-order finite difference differentiation of the periodic function $e^{\sin x}$ are shown.

2.3. Chebyshev spectral collocation formulation

The background of preferable usage of the spectral differentiation methods versus the finite difference differentiation has been discussed extensively, e.g. in [2]. As can be seen in Eqs. (9) and (10), finite difference differentiation results in a sparse banded differentiation matrix, and an increase in the order of approximation will lead to increasing bandwidth. Taking this process to the limit while utilizing unevenly spaced gridpoints (instead of evenly spaced ones as in finite differences) is the

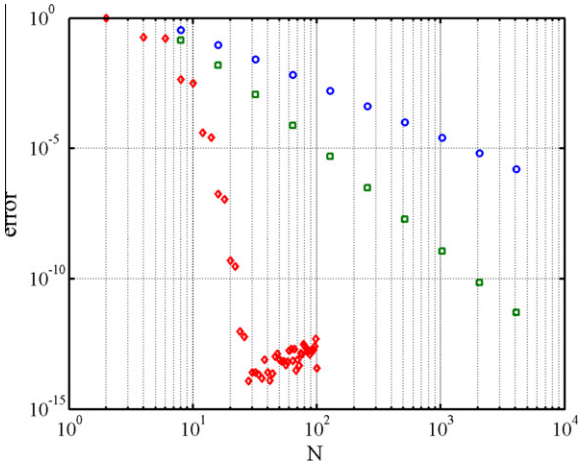

Fig. 1. Comparison of convergence of second-order (circles) and fourth-order (squares) finite differences and spectral differentiation (diamonds) of the function $e^{\sin x}$.

main idea of using spectral methods. Thus we generally work with dense matrices rather than with sparse ones. It is clear, however, that in practice one does not work with infinite matrices such as $\mathscr{A}$ in Eq. (2), so the main steps in the spectral differentiation are setting up an (uneven) grid, fitting a certain approximating polynomial through the values of the function evaluated at the grid points, and then differentiating the polynomial and evaluating the result at each grid point as a linear combination of the nodal function values. The main advantage of pseudospectral differencing techniques lies in their "spectrally accurate" exponential convergence characteristics, which are compared to those of the finite difference techniques in Fig. 1. It can be seen that the errors decrease much faster in the case of spectral differentiation, and their growth after falling below 10^{-14} is due to the rounding errors which now take over. In the remainder of this section, we describe how Chebyshev collocation is used to perform the spectral differentiation.

The Chebyshev collocation points are unevenly spaced points in the domain $[-1,1]$ corresponding to the extremum points of the Chebyshev polynomial of the first kind [6] of degree N. As seen in Fig. 2a, we can also define these points as the projections of equispaced points on the upper half of the unit circle as $t_j = \cos(j\pi/N)$, $j = 0,1,\ldots,N$ where the number of collocation points used is $m = N+1$. A spectral differentiation matrix for the Chebyshev collocation points is obtained by interpolating a polynomial through the collocation points, differentiating that polynomial, and then evaluating the resulting polynomial at the collocation points [8]. We can find the differentiation matrix $\mathbf{D}$ for any order m as follows: let the rows and columns of the $m \times m$ Chebyshev spectral differentiation matrix $\mathbf{D}$ be indexed from 0 to N. The entries of this matrix are

$$\begin{aligned} &D_{00} = \tfrac{2N^2+1}{6}, \quad D_{NN} = -\tfrac{2N^2+1}{6} \\ &D_{jj} = \tfrac{-t_j}{2(1-t_j^2)}, \quad j = 1,\ldots,N-1 \\ &D_{ij} = \tfrac{c_i(-1)^{i+j}}{c_i(t_i-t_j)}, \quad i \neq j,\ i,j = 0,\ldots,N, \quad c_i = \begin{cases} 2, & i = 0,N \\ 1, & \text{otherwise} \end{cases} \end{aligned} \tag{11}$$

The dimension of $\mathbf{D}$ is $m \times m$. Also let the $mq \times mq$ differential operator $\mathbb{D}$ (corresponding to q first order DDEs) be defined as $\mathbb{D} = \mathbf{D} \otimes I_q$, where I_q is a $q \times q$ identity matrix.

A finite-dimensional approximation to $\mathscr{y}(t)$ is now defined as

$$\mathbf{y}(t) = \begin{bmatrix} \mathbf{x}^{\mathrm{T}}(t) & \cdots & \mathbf{x}^{\mathrm{T}}(t-\tau) \end{bmatrix}^{\mathrm{T}} = \begin{bmatrix} \mathbf{x}^{\mathrm{T}}(t_0) & \mathbf{x}^{\mathrm{T}}(t_1) & \mathbf{x}^{\mathrm{T}}(t_2) & \cdots & \mathbf{x}^{\mathrm{T}}(t_N) \end{bmatrix}^{\mathrm{T}} = \begin{bmatrix} \mathbf{y}_1^{\mathrm{T}}(t) & \mathbf{y}_2^{\mathrm{T}}(t) & \mathbf{y}_3^{\mathrm{T}}(t) & \cdots & \mathbf{y}_m^{\mathrm{T}}(t) \end{bmatrix}^{\mathrm{T}} \tag{12}$$

where $\mathbf{x}(t_0) = \mathbf{x}(t)$ and $\mathbf{x}(t_N) = \mathbf{x}(t-\tau)$. (See Fig. 2b and compare to the analogous case in Eq. (7). Equation (2) is now approximated as

$$\dot{\mathbf{y}}(t) = \widehat{\mathbf{A}}_{\mathrm{ch}}\mathbf{y}(t) \tag{13}$$

where $\widehat{\mathbf{A}}_{\mathrm{ch}}$ is obtained from $\mathbb{D}$ by (1) replacing the first q rows by zeros and (2) replacing the $q \times q$ left upper corner by $\mathbf{A}$ matrix and the $q \times q$ right upper corner by $\mathbf{B}$ matrix. Thus, the Eq. (13) is as follows (compare to Eqs. (8)–(10))

$$\begin{bmatrix} \dot{\mathbf{y}}_1(t) \\ \dot{\mathbf{y}}_2(t) \\ \vdots \\ \dot{\mathbf{y}}_m(t) \end{bmatrix} = \begin{bmatrix} \mathbf{A} & \mathbf{0}_q & \cdots & \mathbf{0}_q & \mathbf{B} \\ & & \frac{2}{\tau}\left[\mathbb{D}^{(q+1,mq)}\right] & & \end{bmatrix} \begin{bmatrix} \mathbf{y}_1(t) \\ \mathbf{y}_2(t) \\ \vdots \\ \mathbf{y}_m(t) \end{bmatrix} \tag{14}$$

where the superscript $(q+1,mq)$ on $\mathbb{D}$ refers to the fact that only rows of $\mathbb{D}$ between $q+1$ and mq are written into the remaining $(m-1)q \times mq$ part of matrix $\widehat{\mathbf{A}}_{\mathrm{ch}}$. Note that the $2/\tau$ factor in front of the portion of $\mathbb{D}$ above accounts for the fact of rescaling the standard collocation expansion interval $[-1,1]$ to $[0,\tau]$.

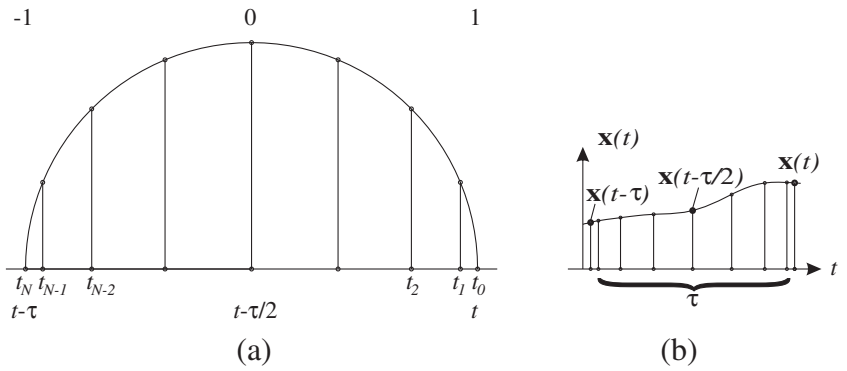

Fig. 2. Diagrams of (a) Chebyshev collocation points as defined by projecting the equispaced points on unit circle onto the horizontal axis and (b) solution $\mathbf{x}(t)$ discretized by Chebyshev spectral CTA.

2.4. Convergence estimates for ChSCTA

The estimate of the error bounds for the collocation polynomial and characteristic roots of constant-coefficient DDEs using Chebyshev collocation points was made in [1]. First, for the closed ball $B(\lambda,\rho)$ in $\mathbb{C}$ for eigenvalue λ of $\mathscr{A}$ and of radius ρ, the upper bound of the error of the collocation polynomial of degree N was found as

$$e_{max} \leqslant \frac{C_0}{\sqrt{N}}\left(\frac{C_1}{N}\right)^N |\phi| \tag{15}$$

where C_0 and $C_1 = \tau(|\lambda| + \rho)e$ are constants independent of N and ϕ is the initial function.

Second, the maximum error of a simple eigenvalue λ^* of the approximate matrix $\widehat{\mathbf{A}}_{\text{ch}}$ is estimated as

$$\max|\lambda^* - \lambda| \leqslant \frac{C_2}{\sqrt{N}}\left(\frac{C_1}{N}\right)^N \tag{16}$$

where C_1 is as defined above and C_2 is a constant independent of N. The spectral accuracy of the Chebyshev collocation technique is observed in Eqs. (15) and (16).

2.5. Examples

2.5.1. First-order scalar DDE

Consider the following scalar DDE with constant coefficients

$$\dot{x}(t) = -ax(t) - bx(t-\tau) \tag{17}$$

Assuming the solution in the form $x(t) = e^{\lambda t}$ yields the characteristic equation

$$\lambda + a + be^{-\lambda\tau} = 0 \tag{18}$$

The stability boundaries for the scalar DDE can be obtained analytically [20] by assuming $\lambda = 0$ as

$$a + b = 0 \tag{19}$$

and also by assuming $\lambda = i\omega$ and separating the real and imaginary parts to obtain the parametric boundary

$$a = \frac{-\omega\cos\tau\omega}{\sin\tau\omega}, \quad b = \frac{\omega}{\sin\tau\omega} \tag{20}$$

The number of the first order equations equals one in this case, so matrices $\mathbf{A}(t) = -a$ and $\mathbf{B}(t) = -b$ in Eq. (14) are constant scalar parameters. For comparison purposes, the constant matrices $\widehat{\mathbf{A}}_{\text{fd}}$ and $\widehat{\mathbf{A}}_{\text{ch}}$ in Eqs. (9), (10) or (14) for this example with $m = 4$ collocation points, $N = 3$ finite differences (we are using $m \neq N$ in order to compare matrices of the same dimension), and $\tau = 1$ are given by

$$\widehat{\mathbf{A}}^c_{\text{fd}} = \begin{bmatrix} -a & 0 & 0 & -b \\ 1.5 & 0 & -1.5 & 0 \\ 0 & 1.5 & 0 & -1.5 \\ 0 & 0 & 3 & -3 \end{bmatrix} \tag{21}$$

$$\widehat{\mathbf{A}}^f_{\text{fd}} = \begin{bmatrix} -a & 0 & 0 & -b \\ 4 & -4 & 0 & 0 \\ 0 & 4 & -4 & 0 \\ 0 & 0 & 4 & -4 \end{bmatrix} \tag{22}$$

$$\widehat{\mathbf{A}}_{\text{ch}} = \begin{bmatrix} -a & 0 & 0 & -b \\ 2 & -2/3 & -2 & 2/3 \\ -2/3 & 2 & 2/3 & -2 \\ 1 & -8/3 & 8 & -19/3 \end{bmatrix} \tag{23}$$

Stability of the equilibrium solution of Eq. (17) is determined by eigenvalues of the two $\widehat{\mathbf{A}}$ matrices, and it is the left half plane stability, i.e. the spectral abscissa $\alpha(\widehat{\mathbf{A}})$ must be less than zero for asymptotic stability. Four stability boundaries are shown in Fig. 3 for $\tau = 1$. The dots indicate the plot of the curves in Eqs. (19) and (20), thin solid line represents the stability chart obtained by the proposed method, the thick dashed line is the stability boundary obtained by CTA using central finite differences described in [3], and the dash-dotted line is used for the forward finite difference boundary. It can be seen in the figure and on the blow-up that already for five collocation points the stability boundary obtained by ChSCTA exactly matches the analytical parametric boundary curve of Eq. (20), whereas the boundaries resulting from the finite difference CTA do not, the central finite difference-based boundary being closer to the exact stability boundary than the forward finite difference-based one.

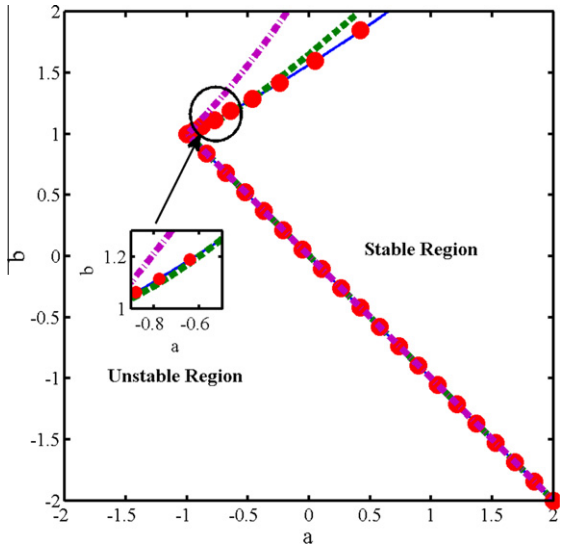

Fig. 3. Diagrams of stability of the scalar DDE (17) for $\tau = 1$ obtained analytically (dotted), by ChSCTA (solid), CTA involving centered finite differences from [3] (dashed), and forward finite differences (dash-dotted). Five collocation points and four finite differences were used to keep the same dimension of $\widehat{\mathbf{A}}_{\mathrm{ch}}$, $\widehat{\mathbf{A}}_{\mathrm{fd}}^{c}$, and $\widehat{\mathbf{A}}_{\mathrm{fd}}^{f}$ matrices.

This lets us again conclude that the method based on Chebyshev collocation is more accurate than the finite difference formulation.

Another way to check how well the approximation agrees with the exact solution is to compute the first m roots of the transcendental characteristic equation (18) and compare them to the eigenvalues of the $\widehat{\mathbf{A}}_{\mathrm{ch}}$ and $\widehat{\mathbf{A}}_{\mathrm{fd}}$ matrices. This comparison is shown in Fig. 4 for the point $(a,b) = (1.5,1)$ for (a), (c), (e) $m = 20$ and (b), (d), (f) $m = 40$ collocation points. It is seen that for $m = 20$ collocation points, the first eight eigenvalues of $\widehat{\mathbf{A}}_{\mathrm{ch}}$ match the corresponding roots of characteristic equation, whereas only one pair of complex conjugate eigenvalues of $\widehat{\mathbf{A}}_{\mathrm{fd}}$ barely matches the pair of roots of characteristic equation with the greatest real part. In the $m = 40$ collocation points case, the number of eigenvalues of $\widehat{\mathbf{A}}_{\mathrm{ch}}$ matching the roots of characteristic equation increases to 18. The number of eigenvalues of $\widehat{\mathbf{A}}_{\mathrm{fd}}$ which are close to the roots of characteristic equation does not change once m is increased. Therefore, while ChSCTA captures the dominant eigenvalues of the system much better than do finite differences, those corresponding to higher frequencies are missed.

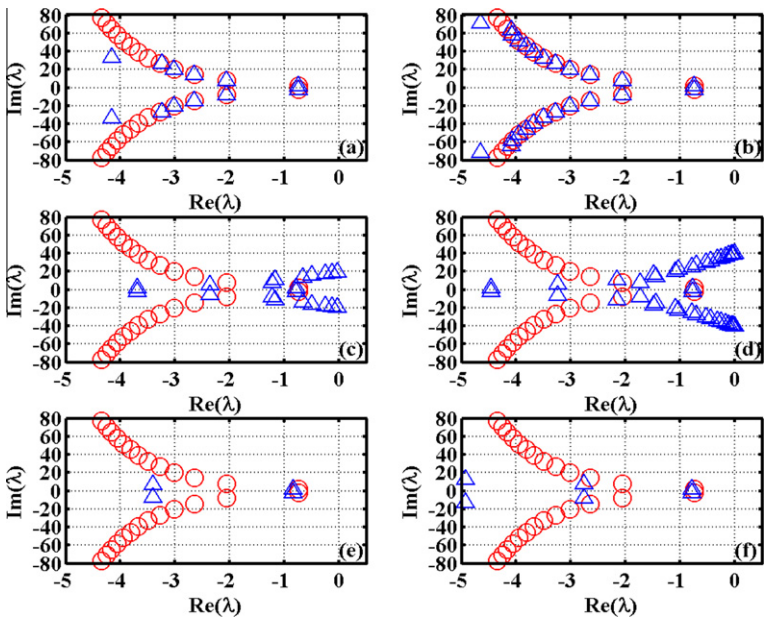

Fig. 4. Eigenvalues of Eq. (17) for the point $(a,b) = (1.5,1)$ obtained by solving Eq. (18) numerically (circles) and computed directly from matrices $\widehat{\mathbf{A}}_{\mathrm{ch}}$ (triangles, first row) and $\widehat{\mathbf{A}}_{\mathrm{fd}}^{c}$ and $\widehat{\mathbf{A}}_{\mathrm{fd}}^{f}$ (triangles, second and third rows, respectively). (a), (c), (e) $m = 20$, $N = 19$ and (b), (d), (f) $m = 40$, $N = 39$.

2.5.2. Second-order DDE with constant coefficients

Consider the second-order DDE with constant coefficients

$$\ddot{x}(t) + ax(t) = cx(t - 2\pi) \tag{24}$$

In this case, the approximation from Eq. (14) is given by setting $\mathbf{A} = \begin{bmatrix} 0 & 1 \\ -a & 0 \end{bmatrix}$ and $\mathbf{B} = \begin{bmatrix} 0 & 0 \\ c & 0 \end{bmatrix}$ in Eq. (14). Just like in the previous example, here we are dealing with left half plane stability. The stability diagram of second-order DDE with constant coefficients approximated by ChSCTA and by CTA using finite differences is shown in Fig. 5 along with the exact stability boundaries obtained first in [21] and shown in [22]. It can be seen that the lines from ChSCTA approximation and the exact stability boundaries are almost identical, whereas the stability boundary obtained by the finite difference approximation starts to significantly deviate from the exact one beyond $a = 0.625$, this deviation being greater for forward compared to the central finite differences. Again, the finite difference approximation shows less accuracy compared to ChSCTA.

3. Continuous time approximation for periodic DDEs

3.1. ChSCTA formulation

In this section, we will be following the same *numerical* procedure to perform the ChSCTA of the time-periodic analogue of Eq. (1), i.e.

$$\begin{aligned} \dot{\mathbf{x}}(t) &= \mathbf{A}(t)\mathbf{x}(t) + \mathbf{B}(t)\mathbf{x}(t - \tau) \\ \mathbf{x}(t) &= \phi(t), \quad -\tau \leqslant t \leqslant 0 \end{aligned} \tag{25}$$

where $\mathbf{A}(t + T) = \mathbf{A}(t)$ and $\mathbf{B}(t + T) = \mathbf{B}(t)$. Without a formal justification for doing so, we proceed as in the case of constant coefficients by discretizing a periodic analogue of the operator in Eq. (2). As was noted in the introduction, we assume that such a periodic "infinitesimal operator" $\mathscr{A}(t)$ exists for the purpose of our numerical examples while not focusing on proving its existence. (The reader is referred to the Appendix for an informal theoretical justification).

Eq. (14) thus becomes

$$\begin{bmatrix} \dot{\mathbf{y}}_1(t) \\ \dot{\mathbf{y}}_2(t) \\ \vdots \\ \dot{\mathbf{y}}_m(t) \end{bmatrix} = \begin{bmatrix} \mathbf{A}(t) & \mathbf{0}_q & \cdots & \mathbf{0}_q & \mathbf{B}(t) \\ & & \frac{2}{\tau}\left[\mathbb{D}^{(q+1,mq)}\right] & & \end{bmatrix} \begin{bmatrix} \mathbf{y}_1(t) \\ \mathbf{y}_2(t) \\ \vdots \\ \mathbf{y}_m(t) \end{bmatrix} \tag{26}$$

Therefore, it is hypothesized that Eq. (26) can be used to obtain both time response and stability properties of Eq. (25). For the purpose of stability analysis, Eq. (26) is numerically integrated mq times with initial conditions $[1\ 0\ 0 \cdots 0]^{\mathrm{T}}$, $[0\ 1\ 0 \cdots 0]^{\mathrm{T}}$ etc. from zero to T in order to form the $mq \times mq$ monodromy matrix $U = \Phi(T)$. The final values of the state vector after integration form the columns of the matrix whose eigenvalues (Floquet multipliers) determine the stability by the unit circle criterion, i.e. if all eigenvalues have magnitude less than one (the spectral radius $\rho(\Phi(T)) < 1$), the system is asymptotically stable. Once the magnitude of the greatest eigenvalue becomes greater than one due to variation of system parameters, the system loses stability. Obviously, this technique is not an efficient method for stability analysis compared to computing the

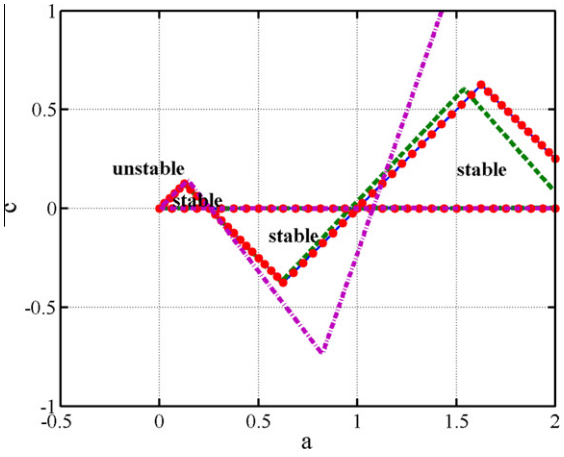

Fig. 5. Stability diagrams of the second-order DDE (27) with constant coefficients (dotted) shown in [22] compared to the ones obtained by ChSCTA (solid) and CTA involving central (dashed) and forward (dash-dotted) finite difference differentiation. 20 collocation points and 19 finite differences were used.

monodromy operator directly; however, the following examples show that the stability of Eq. (25) is preserved in Eq. (26) as long as a sufficient number of collocation points are utilized, while other advantages are discussed later.

Note that convergence estimates in Eqs. (15) and (16) only apply to the constant-coefficient case, while for the periodic case the result of Theorem 1 from [8] provides an *a posteriori* bound for the approximated Floquet multipliers. In addition, one of the following examples shows how a nonlinearity can be accommodated in the formulation.

3.2. Examples

3.2.1. Mathieu's equation with time delay

Consider a second-order periodic DDE, the delayed Mathieu's equation

$$\ddot{x}(t) + (a + b\cos t)x(t) = cx(t - 2\pi) \tag{27}$$

The original version of Mathieu's equation did not contain a time delay and was first discussed in 1868 by Mathieu [23] in his study of the vibration of an elliptical membrane.

First, we treat the regular Mathieu's equation obtained by setting $c = 0$ in Eq. (27). In Eq. (14), $\mathbf{A}(t) = \begin{bmatrix} 0 & 1 \\ -a - b\cos t & 0 \end{bmatrix}$ and $\mathbf{B} = \begin{bmatrix} 0 & 0 \\ 0 & 0 \end{bmatrix}$ so that matrix $\widehat{\mathbf{A}}_{\mathrm{ch}}(t)$ in Eq. (26) is now a periodic matrix. This example is considered in order to obtain a stability diagram which is already known [24]. In Fig. 6, the stability chart obtained by ChSCTA is shown. We compare the ChSCTA results to the results obtained by using the eigenvalues of the monodromy matrix calculated by numerically integrating Mathieu's equation in the state space form from zero to 2π with the initial conditions of $[1\ 0]^T$ and $[0\ 1]^T$. The results obtained by the two methods match well.

The full delayed Mathieu's equation (27) can be approximated by setting $\mathbf{A}(t)$ = the same as above and $\mathbf{B} = \begin{bmatrix} 0 & 0 \\ c & 0 \end{bmatrix}$, so that matrix $\widehat{\mathbf{A}}_{\mathrm{ch}}(t)$ is again periodic. Stability of delayed Mathieu's equation was investigated by Insperger and Stépán in [22]. In Figs. 7 and 8, the stability charts of this equation are given for $c = -0.1$ and $c = 0.1$. The chosen method to compare to is now the Chebyshev Collocation Method (ChCM) used in [8,7]. It can be seen that the stability charts obtained by both methods are almost identical.

3.2.2. A parametrically forced nonlinear DDE

Now consider the formulation of ChSPCTA for nonlinear DDEs. We consider an equation similar to that in [3] with cubic nonlinearity but with parametric sinusoidal excitation (instead of external excitation) as

$$\begin{aligned} &\dot{x}(t) = -ax(t) - bx(t - \tau) - \varepsilon x^3(t) + fx(t)\sin(\omega t) \\ &x(t) = \phi(t), \quad -\tau \leqslant t \leqslant 0 \end{aligned} \tag{28}$$

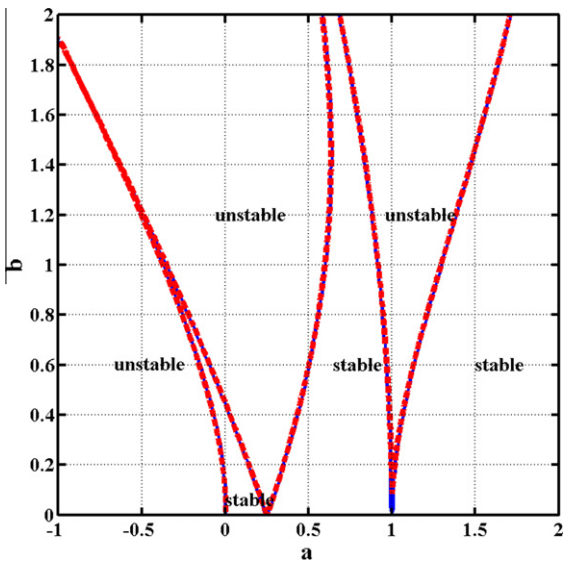

Fig. 6. Stability diagrams of Mathieu's equation (with no delay) produced by computing the eigenvalues of the monodromy matrix obtained by multiple numerical integrations of the periodic ODE system resulting from the discretization by ChSCTA using 20 collocation points (solid) and by two numerical integrations of Mathieu's equation in the state-space form (dots). The results are (almost) indistinguishable.

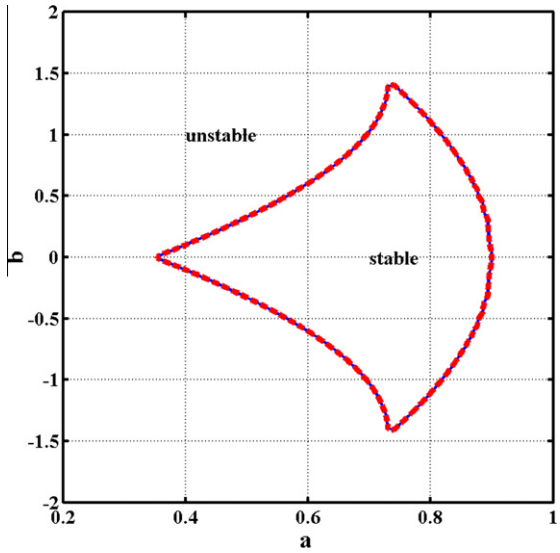

Fig. 7. Diagrams of stability of the delayed Mathieu's equation for $c = -0.1$ obtained by ChSCTA (solid) and by ChCM (dots) with 20 and 50 collocation points used, respectively. The results are indistinguishable.

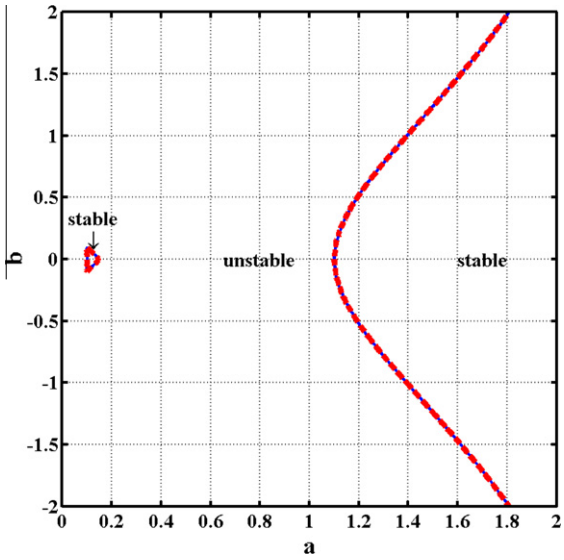

Fig. 8. Diagrams of stability of the delayed Mathieu's equation for $c = 0.1$ obtained by ChSCTA (solid) and by ChCM (dots) with 20 and 50 collocation points used, respectively. The results are indistinguishable.

Eq. (26) for this case is written as

$$\begin{bmatrix} \dot{y}_1(t) \\ \dot{y}_2(t) \\ \vdots \\ \dot{y}_m(t) \end{bmatrix} = \begin{bmatrix} -a + f\sin(\omega t) & 0 & \cdots & 0 & -b \\ & \left[\frac{2}{\tau}\mathbb{D}^{(2,m)}\right] & & & \end{bmatrix} \begin{bmatrix} y_1(t) \\ y_2(t) \\ \vdots \\ y_m(t) \end{bmatrix} - \begin{bmatrix} 1 \\ 0 \\ \vdots \\ 0 \end{bmatrix}^T \varepsilon y_1^3(t) \tag{29}$$

In Fig. 9, the comparison of time series obtained by integration of Eqs. (28) and (29) is shown, and the results are indistinguishable.

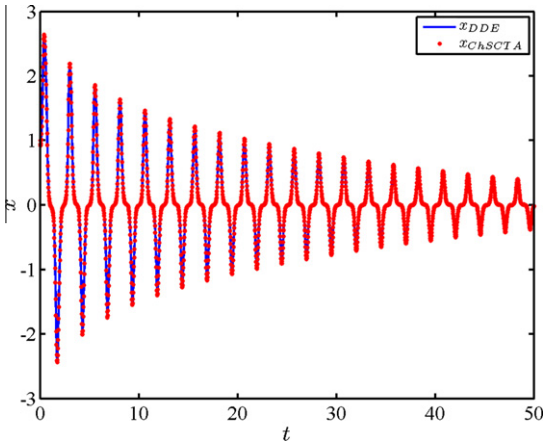

Fig. 9. Time series obtained by integration of Eqs. (28) (solid) and (29) (dashed) for the case of $a = 1.5$, $b = 0.5$, $\varepsilon = 1$, $f = 10$, and $\omega = 5$. The results are indistinguishable.

4. Formulation for linear DDEs with multiple delays

4.1. General formulation

Consider the linear constant or periodic DDE with multiple discrete delays

$$\dot{\mathbf{x}}(t) = \mathbf{A}(t)\mathbf{x}(t) + \sum_{i=1}^{k} \mathbf{B}_i(t)\mathbf{x}(t-\tau_i) \tag{30}$$

such that $\tau_1 < \tau_2 < \cdots < \tau_k$ and $\mathbf{A}(t)$ and $\mathbf{B}_i(t)$ have the same dimensions as in (25). Application of the proposed approach, as discussed in [1], can be made by considering one of the two alternatives. The first alternative is to fit a single Chebyshev polynomial through the entire delay interval $[t-\tau_k, t]$. In this case, placement of matrices $\mathbf{B}_i(t)$, $i < k$, in the first q rows of matrix $\widehat{\mathbf{A}}_{\mathrm{ch}}(t)$ can be done as follows. The interval $[0, \tau_k]$ is first expanded in Chebyshev points. The number of points needed can be determined by comparing each delay τ_i with each element of the expanded interval assuming the certain tolerance. If the values of q elements of the interval lie within the tolerance then their indices form an index interval to place the $q \times q$ $\mathbf{B}_i(t)$ matrix. If the number of indices found is less than q, the number of points is increased and the procedure is repeated. For this purpose, the vector

$$\begin{aligned}\mathbf{y}(t) &= \begin{bmatrix}\mathbf{x}^{\mathrm{T}}(t) & \dots & \mathbf{x}^{\mathrm{T}}(t-\tau_1) & \cdots & \mathbf{x}^{\mathrm{T}}(t-\tau_2) & \cdots & \mathbf{x}^{\mathrm{T}}(t-\tau_k) & \end{bmatrix}^{\mathrm{T}} \\ &= \begin{bmatrix}\mathbf{x}^{\mathrm{T}}(t_0) & \cdots & \mathbf{x}^{\mathrm{T}}(t_{r_1}) & \cdots & \mathbf{x}^{\mathrm{T}}(t_{r_2}) & \cdots & \mathbf{x}^{\mathrm{T}}(t_N) & \end{bmatrix}^{\mathrm{T}} = \begin{bmatrix}\mathbf{y}_1^{\mathrm{T}}(t) & \mathbf{y}_2^{\mathrm{T}}(t) & \mathbf{y}_3^{\mathrm{T}}(t) & \cdots & \mathbf{y}_m^{\mathrm{T}}(t) & \end{bmatrix}^{\mathrm{T}}\end{aligned} \tag{31}$$

is utilized as a finite-dimensional approximation to $\mathscr{Y}(t)$. Here $r_1, r_2, \ldots, r_{k-1}$ are the indices of the Chebyshev points in the expanded interval such that $t_{r_1} = \tau_1, t_{r_2} = \tau_2, \ldots, t_{r_{k-1}} = \tau_{k-1}$. Therefore, using the first alternative, Eq. (30) is approximated as

$$\dot{\mathbf{y}}(t) = \begin{bmatrix}\mathbf{A}(t) & \mathbf{0}_q \dots \mathbf{0}_q & \mathbf{B}_1(t) & \mathbf{0}_q \dots \mathbf{0}_q & \mathbf{B}_2(t) & \dots & \mathbf{B}_{k-1}(t) & \mathbf{0}_q \dots \mathbf{0}_q & \mathbf{B}_k(t) \\ & & & & \left[\frac{2}{\tau_k}\mathbb{D}^{(q+1,mq)}\right] & & & & \end{bmatrix}\mathbf{y}(t) \tag{32}$$

Alternatively, if some of the delays $\tau_1, \tau_2, \ldots, \tau_{k-1}$ do not coincide with Chebyshev points within the expanded interval and it is desired to keep the number of points fixed, Lagrange interpolation can be utilized to place the matrices of coefficients of the delay terms, which now will be multiplied by Lagrange coefficients.

The second alternative to approximate Eq. (30) is to fit a different Chebyshev polynomial of degree N_i through every interval $l_i = [t-\tau_i, t-\tau_{i-1}]$, $i = 1, \ldots, k$. Let the collocation vector on this interval be

$$\mathbf{y}_i(t) = \begin{bmatrix}\mathbf{y}_{i0}^{\mathrm{T}}(t) & \cdots & \mathbf{y}_{iN_i}^{\mathrm{T}}(t) & \end{bmatrix}^{\mathrm{T}} = \begin{bmatrix}\mathbf{x}^{\mathrm{T}}(t-\tau_{i-1}) & \cdots & \mathbf{x}^{\mathrm{T}}(t-\tau_i)\end{bmatrix}^{\mathrm{T}}, \quad i = 1, \ldots, k \tag{33}$$

and $\mathbf{y}_{iN}(t) = \mathbf{y}_{i+1\,0}(t)$, $i = 1, \ldots, k-1$. The extended state vector for the entire interval $[t-\tau_k, t]$ has dimension $q(1+\sum_{i=1}^{k} N_i)$ and is thus written as

$$\mathbf{y}(t)=\begin{bmatrix}\mathbf{y}_{10}(t)\\ \vdots\\ \mathbf{y}_{1N_1}(t)=\mathbf{y}_{20}(t)\\ \vdots\\ \mathbf{y}_{k-1\ N_{k-1}}(t)=\mathbf{y}_{k\ 0}(t)\\ \vdots\\ \mathbf{y}_{kN_k}(t)\end{bmatrix} \tag{34}$$

Then the approximation to (30) using the second alternative can be obtained as

$$\dot{\mathbf{y}}(t)=\begin{bmatrix}\mathbf{A}(t)\ \mathbf{0}_q\ldots\mathbf{0}_q\ \mathbf{B}_1(t)\ \mathbf{0}_q\ldots\mathbf{0}_q\ \mathbf{B}_2(t)\ \cdots\ \mathbf{B}_{k-1}(t)\ \mathbf{0}_q\ldots\mathbf{0}_q\ \mathbf{B}_k(t)\\ \left[\ \frac{2}{|l_1|}\mathbb{D}^{\ (q+1,m_1q)}\ \right]\\ \left[\ \frac{2}{|l_2|}\mathbb{D}^{\ (q+1,m_2q)}\ \right]\\ \left[\ \ddots\right.\\ \left.\ddots\ \right]\\ \left[\ \frac{2}{|l_k|}\mathbb{D}^{\ (q+1,m_kq)}\ \right]\end{bmatrix}\mathbf{y}(t) \tag{35}$$

where $|l_i|=\tau_i-\tau_{i-1}$ denotes the length of each interval l_i and $m_i=N_i+1$. In the case that the polynomial degrees N_i are the same (say N), the size of $\widehat{\mathbf{A}}_{\rm ch}(t)$ matrix is $q(kN+1)\times q(kN+1)$. Even though the size of $\widehat{\mathbf{A}}_{\rm ch}(t)$ matrix is greater in this case, the second alternative avoids the evaluation of Lagrange coefficients at the discrete delay points when forming the first q rows since these are always mesh points. For the greater number of delays, this advantage clearly increases and, moreover, we can utilize the fact that the approximate matrix is sparse for large k.

4.2. Examples

4.2.1. Constant-coefficient DDE with two delays

Consider the linear scalar DDE with two fixed time delays

$$\dot{x}(t)=-ax(t)-bx(t-\tau_2)-cx(t-\tau_1) \tag{36}$$

We choose $\tau_1=1/2$ and $\tau_2=1$ and compare the results to those for Eq. (17). Introducing vector

$$\mathbf{y}(t)=[x(t)\quad\cdots\quad x(t-\tau_1)\quad\cdots\ x(t-\tau_2)]^{\rm T}=\left[x(t_0)\quad\cdots\quad x(t_{N/2})\quad\cdots\quad x(t_N)\right]^{\rm T} \tag{37}$$

as an expansion of $x(t)$ in the interval $[0,\tau_2]$, the first alternative discussed in the previous section results in the approximation

$$\begin{bmatrix}\dot{y}_1(t)\\ \dot{y}_2(t)\\ \vdots\\ \dot{y}_m(t)\end{bmatrix}=\begin{bmatrix}-a & 0 & \cdots & -c & \cdots & 0 & -b\\ & & & \left[2\mathbb{D}^{(2,m)}\right] & & & \end{bmatrix}\begin{bmatrix}y_1(t)\\ y_2(t)\\ \vdots\\ y_m(t)\end{bmatrix} \tag{38}$$

Note that in this case, the number m of collocation points used should be odd, in order to have the term $y_{N/2}(t)=x(t-1/2)$ corresponding to $-c$ in the exact middle of the top row of $\widehat{\mathbf{A}}_{\rm ch}$. In Fig. 10, the stability chart of Eq. (36) approximated by Eq. (38) is presented in the (a,b) parameter plane for $c=2$ along with the stability chart from Fig. 3. This stability diagram illustrates how the change in c influences stable and unstable regions. The approximation obtained by the second alternative and $N_1=N_2=N$ (i.e. two intervals of collocation points) can be written as

$$\begin{bmatrix}\dot{y}_1(t)\\ \dot{y}_2(t)\\ \vdots\\ \dot{y}_m(t)\end{bmatrix}=\begin{bmatrix}-a\ 0\ \cdots\ -c\ \cdots\ 0\ -b\\ \left[\ 4\mathbb{D}^{(2,m)}\ \right]\\ \left[\ 4\mathbb{D}^{\ (2,m)}\ \right]\end{bmatrix}\begin{bmatrix}y_1(t)\\ y_2(t)\\ \vdots\\ y_m(t)\end{bmatrix} \tag{39}$$

which gives the results which are identical to the ones obtained using the first alternative.

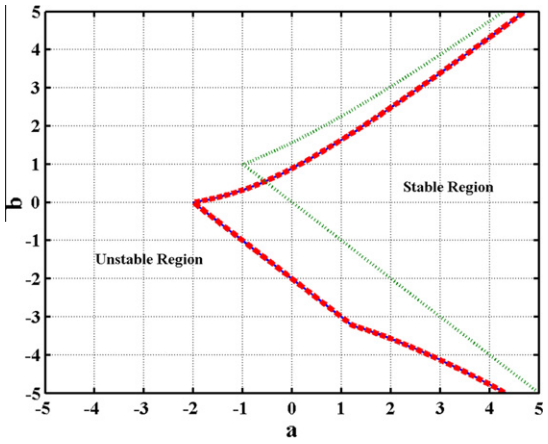

Fig. 10. Stability chart for the linear DDE with two delays, $c = 2$, $\tau_1 = 1/2$, and $\tau_2 = 1$ obtained by ChSCTA (20 collocation points, solid) compared to ChCM (50 collocation points, dashed-indistinguishable) and to the stability chart for $c = 0$.

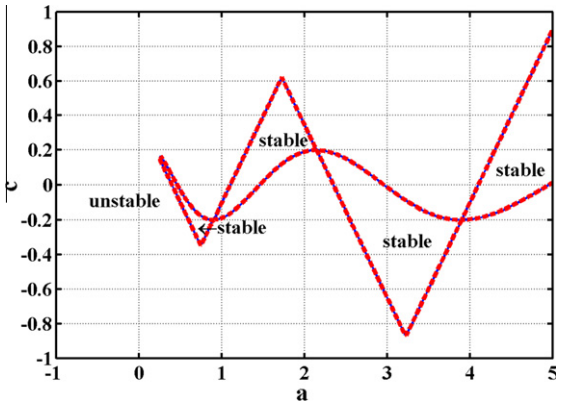

Fig. 11. Stability chart for Mathieu's equation with two delays $b = d = 0.1$ obtained by ChSCTA (20 collocation points, solid) compared to ChCM (50 collocation points, dashed).

4.2.2. Mathieu's equation with two delays

We now apply ChSCTA to an undamped Mathieu's equation with two discrete delays written as

$$\ddot{x}(t) + (a + b\cos t)x(t) = cx(t - 2\pi) + dx(t - 4\pi) \tag{40}$$

For this case, using the second alternative with $m_1 = m_2 = m$, Eq. (35) is written as

$$\dot{\mathbf{y}}(t) = \begin{bmatrix} \mathbf{A}(t)\ \mathbf{0}_2 \ldots \mathbf{0}_2\ \mathbf{B}_1(t)\ \mathbf{0}_2 \ldots \mathbf{0}_2\ \mathbf{B}_2(t) \\ \begin{bmatrix} \frac{1}{\pi}\mathbb{D}^{(3,2m)} \end{bmatrix} \\ \begin{bmatrix} \frac{1}{\pi}\mathbb{D}^{(3,2m)} \end{bmatrix} \end{bmatrix} \mathbf{y}(t) \tag{41}$$

where $\mathbf{A}(t)$ = is defined in Section 3.2.1, $\mathbf{B}_1 = \begin{bmatrix} 0 & 0 \\ c & 0 \end{bmatrix}$, and $\mathbf{B}_2 = \begin{bmatrix} 0 & 0 \\ d & 0 \end{bmatrix}$. The stability chart obtained by ChSCTA superimposed with that obtained by Chebyshev collocation method is shown in Fig. 11.

5. Conclusions

The approximation technique proposed in [1] for discretizing the infinitesimal generator of a system of constant-coefficient DDEs using pseudospectral differencing was extended to the systems of DDEs with periodic coefficients and compared to a finite difference-based continuous time approximation. Specifically, the use of Chebyshev spectral collocation was proposed in order to obtain the "spectral accuracy" convergence behavior shown in [2]. The stability of first and second-order constant-coefficient DDEs with one or two fixed delays, as well as of the delayed Mathieu's equation with one and two discrete delays was studied using the proposed technique. Another example considered was a first order DDE with cubic nonlinearity and parametric sinusoidal excitation. In all the examples, the stability diagrams obtained by the approximation by

the proposed method match well with either the ones obtained analytically, or those obtained before by other methods, such as the Chebyshev collocation method used in [7,8]. The greater accuracy and convergence properties of the investigated method compared to the finite difference-based continuous time approximation described in [3,4] were successfully demonstrated.

Advantages to the proposed technique, as opposed to other pseudospectral methods and other techniques which directly discretize the monodromy operator of a periodic DDE system, include the ability to obtain a continuous response by integrating the resulting periodic ODEs (as opposed to using the approximate monodromy operator with the method of steps), and that, as in [9], no rational relations between the delays and forcing period are necessary for stability analysis. In addition, the method allows for the construction of a Liapunov–Floquet transformation as has been shown theoretically in [25] and which will be shown in the future work.

Acknowledgements

Financial support from NSF Grant No. CMMI-0900289 is gratefully acknowledged. The authors would also like to thank Dr. Ed Bueler for his help in understanding the theoretical nature of the periodic infinitesimal operator.

Appendix A

Here, we offer a possible informal theoretical justification for the numerical method employed for periodic DDEs, specifically the assumption that Eq. (26) yields the same response and stability as Eq. (25), such that a periodic analogue of Eq. (2) exists (which is discretized in Eq. (26)). Consider a periodic system of DDEs with a single discrete time delay described by

$$\begin{aligned}&\dot{\mathbf{x}}(t) = \mathbf{A}(t)\mathbf{x}(t) + \mathbf{B}(t)\mathbf{x}(t-\tau)\\ &\mathbf{x}(t) = \phi(t), \quad -\tau \leqslant t \leqslant 0\end{aligned} \tag{A1}$$

where $\mathbf{x} \in \mathbb{R}^q$ is a q-dimensional state vector, $\mathbf{A}(t+T) = \mathbf{A}(t)$ and $\mathbf{B}(t+T) = \mathbf{B}(t)$ are T-periodic matrices, and $\phi(t)$ is the initial vector function. As in [25], define the two-parameter operator $\Phi(t,\theta)$ as

$$\Phi(t,\theta)\phi(\theta) = \mathbf{x}_t(\theta,\phi), \quad \theta \in [-\tau, 0] \tag{A2}$$

$$\Phi(t,t) = I, \quad \Phi(t,r)\Phi(r,\theta) = \Phi(t,\theta) \tag{A3}$$

and monodromy operator $U = \Phi(T,0)$ such that $U\phi = \mathbf{x}_T(\phi)$. Equations (A3) are the properties of the operator in Eq. (A2) which are analogous to the properties of a semigroup for a constant-coefficient DDE solution operator defined in [13].

Suppose we replace the continuous matrix-valued functions $\mathbf{A}(t)$ and $\mathbf{B}(t)$ by piecewise constant approximations on k intervals of length δ, where $\delta = T/k \ll 1$ is a small positive number. Then for t in a small time interval $[t_*,\ t_* + \delta]$ $\widetilde{\mathbf{A}} = \mathbf{A}(t_*)$, and similarly, $\widetilde{\mathbf{B}} = \mathbf{B}(t_*)$, and Eq. (A1) can be approximated using the constant-coefficient DDE

$$\dot{\mathbf{x}}(t) = \widetilde{\mathbf{A}}\mathbf{x}(t) + \widetilde{\mathbf{B}}\mathbf{x}(t-\tau) \tag{A4}$$

As explained in [14,12,13], Eq. (A4) can be treated as an abstract ODE

$$\dot{\mathscr{y}}(t) = \mathscr{A}^*\mathscr{y}(t) \tag{A5}$$

where $\mathscr{y}(t)$ is an infinite-dimensional vector and $\mathscr{A}^*$ is the infinitesimal generator which satisfies

$$\mathscr{D}(\mathscr{A}^*) = \left\{\phi \in \mathscr{C}([-\tau,0],\mathbb{R}^n) :\ \frac{d\phi}{d\theta} \in \mathscr{C}([-\tau,0],\mathbb{R}^n), \dot{\phi}(0) = \widetilde{\mathbf{A}}\phi(0) + \widetilde{\mathbf{B}}\phi(-\tau)\right\}, \tag{A6}$$

$$\mathscr{A}^*\phi = \frac{d\phi}{d\theta}$$

where $\mathscr{D}(\mathscr{A}^*)$ denotes the domain of $\mathscr{A}^*$ and $\mathscr{C}$ is a Banach space. Considering a sequence of k such infinitesimal generators in the interval $[0,T]$, we obtain a piecewise constant approximation for a periodic "infinitesimal operator" $\mathscr{A}(t) = \mathscr{A}(t+T)$ on the interval $[0,T]$, which becomes a continuous function of t in the limit as $\delta \to 0$. Therefore, for all t Eq. (A5) is written as

$$\dot{\mathscr{y}}(t) = \mathscr{A}(t)\mathscr{y}(t) \tag{A7}$$

Note that even though the operator $\mathscr{A}(t)$ (which is not an infinitesimal generator) depends on time, it acts on the same space $\mathscr{C}([-\tau,0],\mathbb{R}^n)$ as $\mathscr{A}^*$. Approximation of the infinite-dimensional vector $\mathscr{y}(t)$ and operator $\mathscr{A}(t)$ with finite dimensional ones yields Eq. (26).

References

[1] Breda D, Maset S, Vermiglio R. Pseudospectral differencing methods for characteristic roots of delay differential equations. SIAM J Sci Comput 2005;27:482–95.
[2] Trefethen LN. Spectral methods in Matlab. Philadelphia: SIAM Press; 2000.

[3] Sun J-Q. A method of continuous time approximation of delayed dynamical systems. Commun Nonlinear Syst Numer Simul 2009;14:998–1007. doi:10.1016/j.cnsns.2008.02.008.
[4] Sun J-Q, Song B. Control studies of time-delayed dynamical systems with the method of continuous time approximation. Commun Nonlinear Syst Numer Simul 2009;14:3933–44. doi:10.1016/j.cnsns.2009.02.011.
[5] Breda D, Maset S, Vermiglio R. Computing the characteristic roots for delay differential equations. IMA J Numer Anal 2004;24:1–19.
[6] Fox L, Parker IB. Chebyshev polynomials in numerical analysis. London: Oxford University Press; 1968.
[7] Butcher EA, Bobrenkov OA, Bueler E, Nindujarla P. Analysis of milling stability by the Chebyshev collocation method: algorithm and optimal stable immersion levels. J Comput Nonlinear Dynam 2009;4:031003.
[8] Bueler E. Error bounds for approximate eigenvalues of periodic-coefficient linear delay differential equations. SIAM J Numer Anal 2007;45(6):2510–36.
[9] Breda D, Maset S, Vermiglio R. Numerical computation of characteristic multipliers for linear time-periodic delay differential equations. In: Proceedings of the sixth IFAC workshop on linear time-delay systems, L'Aquila, Italy; 2006.
[10] Insperger T, Stépán G. Semi-discretization method for delayed systems. Int J Numer Methods Eng 2002;55(5):503–18.
[11] Bayly PV, Halley JE, Mann BP, Davis MA. Stability of interrupted cutting by temporal finite element analysis. J Manuf Sci Eng 2003;125:220–5.
[12] Bátkai A, Piazzera S. Semigroups for delay equations. Research notes in mathematics, vol. 10. Wellesley, MA: A K Peters Ltd.; 2005.
[13] Michiels W, Niculescu S-I. Stability and stabilization of time-delay systems: an eigenvalue-based approach. Philadelphia: SIAM Press; 2008.
[14] Hale JK, Verduyn Lunel S. Introduction to functional differential equations. New York: Springer-Verlag; 1993.
[15] Breda D. Solution operator approximations for characteristic roots of delay differential equations. Appl Numer Math 2006;56:305–17.
[16] Butcher EA, Bobrenkov OA. The Chebyshev spectral continuous time approximation for periodic delay differential equations. In: Proceedings of IDETC/CIE ASME conference, San Diego, CA, USA; 2009.
[17] Bellen A. One-step collocation for delayed differential equations. J Comp Appl Math 1984;10:275–83.
[18] Ito K, Tran HT, Manitius A. A fully-discrete spectral method for delay-differential equations. SIAM J Numer Anal 1991;28:1121–40.
[19] Engelborghs K, Luzyanina T, In 't Hout KJ, Roose D. Collocation methods for the computation of periodic solutions of delay differential equations. SIAM J Sci Comput 2000;22:1593–609.
[20] Niculescu S-I. Delay effects on stability: a robust control approach. London: Springer-Verlag; 2001.
[21] Hsu CS, Bhatt SJ. Stability charts for second order dynamical systems with time lag. J Appl Mech (ASME) 1966;33E(1):119–24.
[22] Insperger T, Stépán G. Stability chart for the delayed Mathieu equation. Proc R Soc Math Physic Eng Sci 2002;458:1989–98.
[23] Mathieu É. Mémoire sur le mouvement vibratoire d'une membrane de forme elliptique. J Math 1868;13:137–203.
[24] Van der Pol F, Strutt MJO. On the stability of the solutions of Mathieu's equation. Philos Mag J Sci 1928;5:18–38.
[25] Diekmann O, van Gils SA, Verduyn Lunel SM, Walther HO. Delay equations – functional, complex and nonlinear analysis. AMS series, 110. New York: Springer-Verlag; 1995.